Estimation of error maps for evaluating precision of myocardial T2* mapping techniques

Christopher M. Sandino[1,2], Peter Kellman[2], Michael S. Hansen[2], Andrew E. Arai[2], and Hui Xue[2]

[1]*Ming Hsieh Department of Electrical Engineering, University of Southern California, Los Angeles, California, United States,* [2]*Lab of Cardiac Energetics, National Heart, Lung, and Blood Institute, Bethesda, Maryland, United States*

Target Audience: Radiologists and MR physicists interested in myocardial tissue iron quantification

Purpose: Pixel-wise T_2* mapping is an emerging clinical technique for detecting iron overload in myocardial tissue. This technique generates a parametric map of T_2* by fitting multi-echo data to a specified signal model to estimate a single T_2* decay constant at each pixel [1]. Pixel-wise mapping offers potential benefits over the well-established ROI-based T_2* mapping technique by providing an intuitive interpretation of data and spatial context between tissues. Saiviroonporn et al. has shown that using pixel-wise maps also reduce intra- and inter-class observer variability when compared to the ROI-based method [2]. However, the precision of pixel-wise T_2* mapping is much lower than its ROI-based counterpart due to its use of relatively lower SNR data. There is on-going research to optimize imaging protocols and signal reconstruction methods to optimize pixel-wise T_2* mapping and improve its robustness to noise [3-5]. In order to evaluate and analyze precision of T_2* mapping techniques, we propose a method to estimate pixel-wise error maps composed of standard deviations (SD) of each T_2* measurement.

Methodology: The signal model used to estimate T_2* is assumed to be a 2-parameter mono-exponential of the form $y(TE) = A^{*}\exp(-TE/T_2^{*})$ where y is signal intensity, TE is echo time, A is amplitude, and T_2* is the transverse decay constant. Observed data is fitted to the signal model using a non-linear downhill simplex algorithm, which minimizes the error of the fit residuals in the least squared sense. The SD is estimated by computing the covariance matrix of model parameters A and T_2* by inverting the first-order approximation of the parameters' Hessian matrix, as formulated by Kellman et al. [6]:

$$C = \begin{bmatrix} \sigma_{T_2^*}^2 & \cdot \\ \cdot & \sigma_A^2 \end{bmatrix} = inv\left(\sum_{i=0}^{N-1} \frac{1}{\sigma_i^2} \begin{bmatrix} \frac{\partial y(TE_i)}{\partial T_2^*}\frac{\partial y(TE_i)}{\partial T_2^*} & \frac{\partial y(TE_i)}{\partial T_2^*}\frac{\partial y(TE_i)}{\partial A} \\ \frac{\partial y(TE_i)}{\partial A}\frac{\partial y(TE_i)}{\partial T_2^*} & \frac{\partial y(TE_i)}{\partial A}\frac{\partial y(TE_i)}{\partial A} \end{bmatrix} \right) \quad \text{[Eqn. 1]}$$

$$\frac{\partial y(TE)}{\partial A} = exp\left(-\frac{TE}{T_2^*}\right) \quad \text{[Eqn. 2]}$$

$$\frac{\partial y(TE)}{\partial T_2^*} = A * exp\left(-\frac{TE}{T_2^*}\right) * \left(\frac{TE}{T_2^{*2}}\right) \quad \text{[Eqn. 3]}$$

Where σ_A^2 and σ_{T2*}^2 are variances of model parameters A and T_2* respectively, and σ_i is the noise variance, which is robustly estimated using the median absolute deviation of the fit residuals [7]. All methods described were implemented in C++ on the Gadgetron platform [8] for inline processing on the scanner. In order to validate this method, the true SD was measured by scanning six iron oxide agarose gel phantoms with a typical T_2* range (3-30 ms) N=64 times and plotted against the estimated SD. In-vivo studies were also performed to evaluate different imaging protocols used for T_2* mapping.

Imaging: Phantom and in-vivo datasets were acquired on a 1.5T clinical scanner (MAGNETOM Aera, Siemens AG, Erlangen, Germany) using a multi-echo GRE sequence with gradient flyback for mono-polar readout with 8 echoes (TE = 1.6, 3.9, 6.2, 8.5, 10.8, 13.2, 15.5, and 17.8 ms and TR = 19.7 ms). The matrix size was 256x144 with typical FOV of 360x270 mm^2 and 8 mm slice thickness. The excitation flip angle was 18°. There were 9 segments acquired each heartbeat. A breath-held, segmented acquisition with ECG triggering was used for both in-vivo and phantom datasets. In-vivo data was acquired using a dark blood preparation, which suppressed strong bloodpool signal and prevented it from contaminating the desired myocardium signal [9].

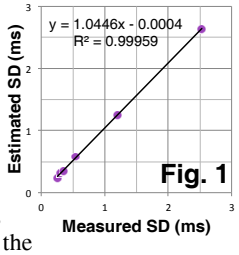

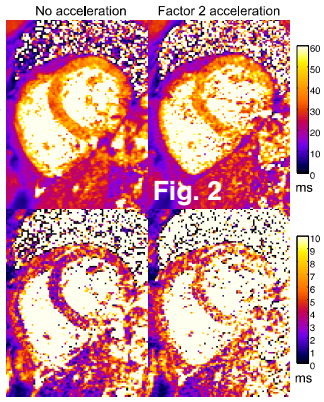

Results & Discussion: Measured and estimated SD's were well correlated, as shown in Fig. 1. SD's for higher T_2* tended to be slightly overestimated likely due to lack of samples of the recovery curve at later echo times. A signal model mismatch occurs where the curve's exponential behavior is not fully characterized, which causes instability in the fitting process. Note that a limitation of this method is that it measures standard deviation due to thermal noise, not physiological noise. In-vivo datasets were acquired to show examples of using SD maps as a quality metric for evaluation of T_2* mapping techniques. Fig. 2 shows a comparison between the SD maps for data acquired with and without parallel imaging acceleration. Note that the SD tended to be higher in tissue further away from the surface coils, as expected. A faster acquisition corresponded to higher SD measurements in the myocardium due to trade-offs between acquisition speed and measurement precision. Fig. 3 shows a comparison between datasets acquired with good and poor breath-holds. A potential clinical application is presented where the SD map is used as a means to mask unreliable pixels with high SD.

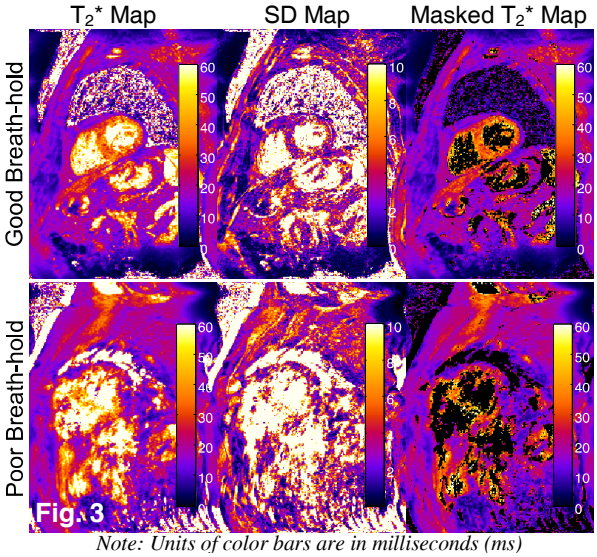

Note: Units of color bars are in milliseconds (ms)

Conclusion: Error (SD) maps can be accurately estimated and used as a quality metric for improving confidence in interpreting images and evaluating protocols of T_2* mapping techniques. Such a tool will be useful for prototyping and optimizing more precise T_2* mapping techniques.

References: [1] Clark PR, et al. Magn Reson Imaging, 2000. [2] Saiviroonporn P, et al. J Comput Assist Tomogr, 2011. [3] He T, et al. J Magn Reson Imaging, 2013. [4] Zaman A, et al. J Magn Reson Imaging, 2014. [5] Pei M, et al. Magn Reson Med, 2014. [6] Kellman P, et al. J Cardiovasc Magn Reson, 2013. [7] DuMouchel WH, et al. Proc. Symp. On Interface, 1989. [8] Hansen MS, et al. Magn Reson Med, 2013. [9] Smith GC, et al. J Cardiovasc Magn Reson, 2011.